

See discussions, stats, and author profiles for this publication at: <https://www.researchgate.net/publication/235766968>

# Magdala harbour sedimentation (Sea of Galilee, Israel), from natural to anthropogenic control

Article in *Quaternary International* · July 2013

DOI: 10.1016/j.quaint.2013.01.032

---

CITATIONS

21

---

READS

2,947

10 authors, including:



**Giovanni Sarti**

University of Pisa

160 PUBLICATIONS 2,513 CITATIONS

SEE PROFILE



**Veronica Rossi**

University of Bologna

104 PUBLICATIONS 1,899 CITATIONS

SEE PROFILE



**Stefano De Luca**

Pontifical Institute of Christian Archaeology, Rome - Vatican City

10 PUBLICATIONS 80 CITATIONS

SEE PROFILE



**Anna Lena**

Unior PhD Alumna

8 PUBLICATIONS 77 CITATIONS

SEE PROFILE



Contents lists available at SciVerse ScienceDirect

## Quaternary International

journal homepage: [www.elsevier.com/locate/quaint](http://www.elsevier.com/locate/quaint)

## Magdala harbour sedimentation (Sea of Galilee, Israel), from natural to anthropogenic control

Giovanni Sarti<sup>a,\*</sup>, Veronica Rossi<sup>b</sup>, Alessandro Amorosi<sup>b</sup>, Stefano De Luca<sup>c</sup>, Anna Lena<sup>c</sup>, Christophe Morhange<sup>d</sup>, Adriano Ribolini<sup>a</sup>, Irene Sammartino<sup>b</sup>, Duccio Bertoni<sup>a</sup>, Gianni Zanchetta<sup>a</sup>

<sup>a</sup> Dipartimento di Scienze della Terra, University of Pisa, Via S. Maria 53, 56126 Pisa, Italy

<sup>b</sup> Dipartimento di Scienze Biologiche, Geologiche e Ambientali, University of Bologna, Italy

<sup>c</sup> Studium Biblicum Franciscanum (Faculty of Biblical Sciences and Archaeology), Magdala Project, Israel

<sup>d</sup> CNRS CEREGE Aix Marseille University, IUF, 13535, Europôle de l'Arbois, Aix-en-Provence, France

### ARTICLE INFO

#### Article history:

Available online xxx

### ABSTRACT

Recent excavations undertaken within the framework of the “Magdala Project” in the ancient city of Magdala/Tarichae, located on the western shore of Sea of Galilee (northern Israel), have unearthed a harbour structure extending for more than 100 m, dating from the late Hellenistic (167–63 BC) to the middle Roman (70–270 AD) period, with well-preserved quays and mooring stones. An integrated (sedimentological, micropalaeontological and archaeological) study of the late Holocene sedimentary succession buried beneath the ancient harbour area reveals the harbour’s main evolutionary stages, shedding new light on the natural *versus* anthropogenic control on sedimentation. Three sedimentary sequences, a few decimeters thick, reflect the recent palaeoenvironmental evolution of the Magdala area. These include: 1) a pre-harbour foundation sequence; 2) a harbour sequence; and 3) a harbour abandonment sequence. Above the natural sandy beachface deposits, subject to wave reworking (pre-harbour facies), the abrupt transition to dark silty sands with high metal concentrations reveals the onset of an anthropogenic control on coastal sedimentation through the construction of harbour structures (harbour facies). The overlying, vertically stacked sand and gravel beach deposits (post-harbour facies), record harbour siltation and abandonment at the transition from the Middle to the Late Roman period (270–350 AD).

© 2013 Elsevier Ltd and INQUA. All rights reserved.

### 1. Introduction

Ancient harbour geoarchaeology has grown in importance during the past few decades, and the interest in this discipline is still quickly growing, providing important information on Holocene coastal stratigraphy, palaeogeography and sea-level change. At the same time, integrated geological studies strongly support archaeological interpretations. Thus, the cooperation between archaeology and geosciences can outstandingly enhance knowledge about harbours as interface between human culture and nature, and as sedimentary archives of both human and

environmental pasts (Reinhardt et al., 1994; Morhange et al., 2001; Sivan et al., 2001; Bruckner et al., 2002; Marriner and Morhange, 2006, 2007). Recent examples of integrated studies from the Mediterranean area include the ancient harbours of Marseille (Morhange et al., 2003), Luni (Bini et al., 2009, 2012; Bisson and Bini, 2012), Rome (Giraudi et al., 2009; Goiran et al., 2010; Bellotti et al., 2011), Beirut (Marriner et al., 2008, in press), Sidon (Marriner and Morhange, 2005; Marriner et al., 2006), Tyre (Marriner et al., 2005), Caesarea Marittima (Reinhardt et al., 1994, 1998; Reinhardt and Raban, 1999), Cyprus (Morhange et al., 2000; Devillers, 2008), Troy (Kraft et al., 2003), Liman Tepe (Goodman et al., 2009) and Alexandra Troas (Feuser, 2011) or Byzantium (Bony et al., 2012). These studies clearly document the tight relationship that exists between harbour evolution (e.g. foundation, siltation, abandonment), natural events (e.g. relative sea-level variations, impact of earthquakes or tsunami) and, obviously, the historical and archaeological evolution of coastal areas. No geoarchaeological studies on strictly lacustrine ancient harbours are available to date, with the exception of the ancient lake of Mareotis

\* Corresponding author.

E-mail addresses: [sarti@dst.unipi.it](mailto:sarti@dst.unipi.it) (G. Sarti), [veronica.rossi4@unibo.it](mailto:veronica.rossi4@unibo.it) (V. Rossi), [alessandro.amorosi@unibo.it](mailto:alessandro.amorosi@unibo.it) (A. Amorosi), [magdalaproject@gmail.com](mailto:magdalaproject@gmail.com) (S. De Luca), [iskenderia@gmail.com](mailto:iskenderia@gmail.com) (A. Lena), [morhange@cerge.fr](mailto:morhange@cerge.fr) (C. Morhange), [ribolini@dst.unipi.it](mailto:ribolini@dst.unipi.it) (A. Ribolini), [irene.sammartino@unibo.it](mailto:irene.sammartino@unibo.it) (I. Sammartino), [bertoni@dst.unipi.it](mailto:bertoni@dst.unipi.it) (D. Bertoni), [zanchetta@dst.unipi.it](mailto:zanchetta@dst.unipi.it) (G. Zanchetta).

(Maryut) in Egypt (Blue and Khalil, 2010; Flaux et al., 2011, 2012), which nonetheless corresponds to a coastal lagoon, rather than a freshwater lake.

Around the Sea of Galilee (also known as Tiberias or Kinneret Lake, Israel; Fig. 1), a site of great importance for the history of Jews, Christians and Muslims, twelve roman to byzantine jetties and small piers have been described at an altitude of about  $212 \pm 1$  m bsl (Nun, 1988; Raban, 1988). Recent excavations at the ancient city of Magdala (see Figs. 1 and 2A for location), headed by Stefano De Luca and assisted by Anna Lena (De Luca, 2010, 2012, in press; Lena, 2012; <http://www.magdalaproject.org/WP/>), have unearthed an extensive and well-preserved harbour structure with seven mooring stones (Figs. 2A–B and 3) at an altitude of 208.32 m bsl. This suggests a lake-level higher than previously reported in the literature (Nun, 1987). The preservation *in situ* of mooring stones constitutes, in freshwater environments, a good tool to reconstruct ancient lake levels. In fact due to the lack of bioerosion or traces of bioindicators on the quay façade, the elevation of the mooring stones, compared with the elevation of the bottom of the landing place, can provide a reference for the level of use of the harbour basin and, consequently, for the level of the lake during

the phases of use of the structures. In the case of the Kinneret, the Magdala harbour facilities are so far the only available archaeological data to determine, from the functional surfaces, the height of the water during the Hellenistic/Roman period.

This paper presents the results of a geoarchaeological study undertaken on the sedimentary succession, including anthropogenic structures, buried beneath the Magdala lacustrine harbour, which experienced a long period of human occupation and cultural history from the Late Hellenistic to Middle Roman period (ca. 167 BC–270 AD). The objectives of this paper are: i) to reconstruct the spatial and temporal evolution of the ancient harbour of Magdala, and ii) to furnish a contribution for the discrimination of natural *versus* anthropogenic factors influencing the sedimentary evolution of ancient Mediterranean harbours.

## 2. The archaeological site of Magdala

### 2.1. Archaeological context

The ancient city of Magdala/Tarichaea (as it is called by the 1st century historian Flavius Josephus) was erected around the 3th

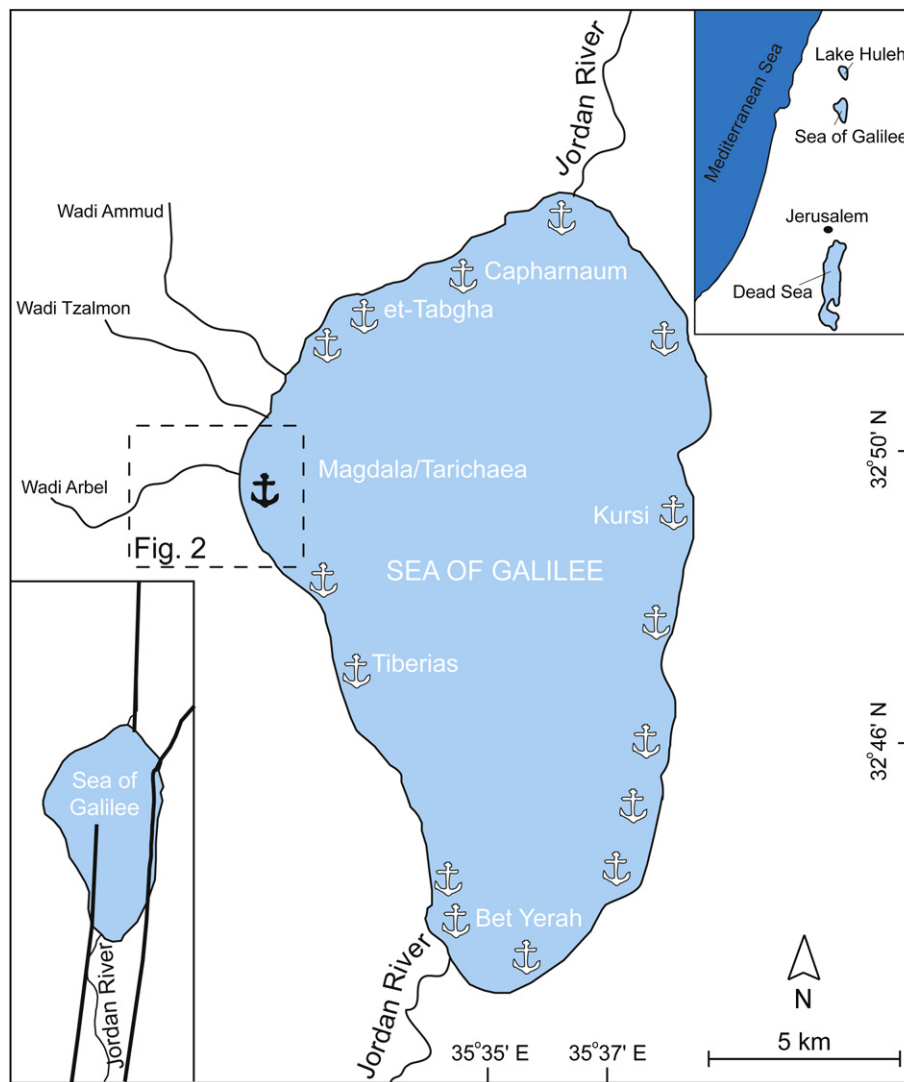


**Fig. 1.** Location of the Sea of Galilee (Israel), with the position of the Roman to Byzantine jetties and small piers recognized by Mendel-Nun (1987) along the lakeshore. The position of Magdala site, in the western part of the Sea of Galilee, is highlighted. The archaeological site of Magdala is shown in greater detail in Fig. 2. On the left: Sea of Galilee, with an indication of the main faults. The bold lines represent the left-lateral Dead Sea transform faults; slightly modified from Marco et al. (2003).

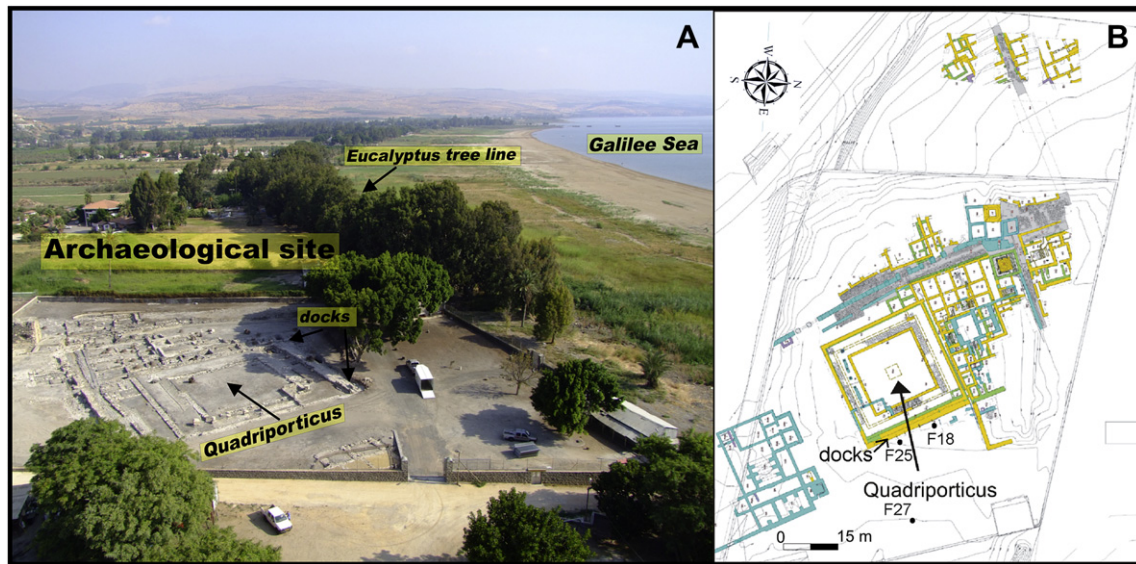


**Fig. 2.** (A) Aerial view of the Magdala area. (B) Plan view of the archaeological site, showing the location of sections F18, F25 and F27 (slightly modified from De Luca, 2010). Different colours highlight distinct historical phases. Green: Hellenistic; yellow: Roman; light blue: Byzantine; purple: Islamic. (For interpretation of the references to colour in this figure legend, the reader is referred to the web version of this article.)

century BC in an ideal position along the western shore of the Sea of Galilee (Fig. 1), crossed by the main trade route connecting Egypt with Damascus and the Galilee Region with the Mediterranean coast. Before the foundation of Tiberias as the capital of Galilee (19 AD), Magdala, which extended over 10 ha, was the main urban centre of the western coast of the Lake. Since Hellenistic times its economic supremacy in the region was very probably related to the activity of an important harbour (De Luca and Lena, *in press*). In this respect, the city's position was likely selected to exploit the direction of the daily westerly winds (the Mediterranean breeze), which generate a counter clockwise circular current on the surface of the lake (Pan et al., 2002), favoring navigation and landing.

The Magdala archaeological site is about 250–300 m far from the present-day lakeshore, at an elevation of 208–206 m bsl (Fig. 2B). The excavations, held four years ago under the auspices of the Studium Biblicum Franciscanum – Faculty of Biblical Sciences and Archaeology of Jerusalem, unearthed a harbour structure formed by two north-south juxtaposed docks (Fig. 3A and B). The first structure, dated on the basis of archaeological findings to the Late Hellenistic period, comprises a huge tower (26 × 17 m) with one of the original mooring stones preserved *in situ* (MS 2) and two sides facing the water. The tower was flanked, to the south, by a quadriporticus (33 × 33 m), which preserves a mooring stone (MS1), also overlooking the stretch of water eastwards and southwards (Fig. 3B).

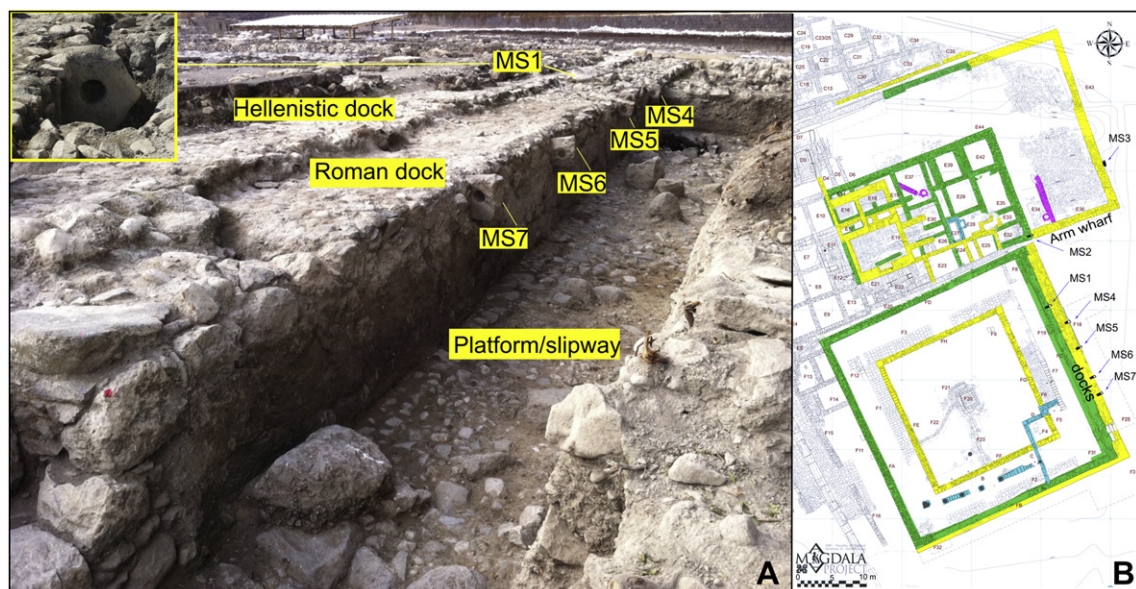


**Fig. 3.** (A) Detailed view of the late Hellenistic and Roman harbour docks and related moorings. MS1 corresponds to the Asmonean mooring, while MS4–7 are mooring stones of Roman age. (B) Whole plan view of the harbour structures (slightly modified from De Luca, 2010), with the location of the moorings (labelled MS1 to MS7). The colours on the map denote distinct historical phases. Green: Hellenistic; yellow: Roman; light blue: Byzantine; purple: Islamic. (For interpretation of the references to colour in this figure legend, the reader is referred to the web version of this article.)

The Roman dock, running along the two sides of the *quadriporticus* and plastered with hydraulic mortar, was built against the Hellenistic wharf. It shows four mooring stones above a slipway, a flight of steps created into the pier, and a platform (13 × 30 m). The latter was built by filling the previous basin along the northern and eastern sides of the Late Hellenistic tower in order to extend the space for landing and, possibly, for loading and unloading boats. The Late Hellenistic and Roman anchorages are approximately at 208 m bsl (208.10 and 208.32 m bsl, respectively).

## 2.2. Geological and geomorphological contexts

The Sea of Galilee is the lowest freshwater lake on Earth, with a total area of 166 km<sup>2</sup> and a maximum average depth of approximately 43 m. The lake is mainly fed by the Jordan River, which flows through it from north to south and, subordinately, by underground springs (Nishri et al., 1999; Hakanson et al., 2000; see Fig. 1). The lake fills a subsiding tectonic depression linked to the activity of the Dead Sea transform, which runs between the Arabic and Sinai plates (Marco et al., 2003, Fig. 1). As a consequence, this area is characterized by strong seismic activity, as documented by three main destructive earthquakes, which occurred in 31 BC, 363 AD and 749 AD, respectively (Russell, 1985; Amiran et al., 1994; Guidoboni, 1994; Marco et al., 2003).

During the late Quaternary, the Sea of Galilee was affected by numerous relative lake-level fluctuations (Hazan et al., 2005). The main lowstands occurred about 42,000, 30,000, 23,800, 13,000 and 8000 cal BP, forcing the lake level down to 240 m bsl. Data from the harbour of Kursi (Raban, 1988), in the eastern part of the Sea of Galilee (see Fig. 1), document that during Late Byzantine times (6th–7th century AD) the lake level reached 214–215 m bsl (Galili et al., 2007). By contrast, highstands, up to 175 m bsl, are documented approximately 39,000, 26,000 and 5000 cal BP, while around 1600 cal BP the lake-level reached 207 m bsl. During the phase of maximum lake-level rise, which took place during the last glacial maximum (26,000–24,000 cal BP; Hazan et al., 2005), a unique body of water, known as Lake Lisan, covered the entire area from the Dead Sea up to the Sea of Galilee and Huleh lake. Therefore, the present Sea of Galilee represents one of the remnant water bodies of the former Late Pleistocene Lake Lisan (Neev and Emery, 1967; Stein, 2001; Hazan et al., 2005). Historical lake-level fluctuations are also recorded and are mainly connected to human-induced modifications (Hambright et al., 2004).

From a geomorphological point of view the settlement of Magdala is located near the lakeshore on the south side of a small alluvial plain of the wadis Arbel, Ammud and Tzalmon, about 8 km wide, slightly dipping towards the lake and bounded by hills made up predominantly of limestones and basalts. These hills are deeply incised and terraced by the modern Arbel, Ammud and Tzalmon wadis (Fig. 1), which previously fed the alluvial plain and the Sea of Galilee. Nowadays, the sedimentary supply from these wadi systems is negligible because of their artificial channelization.

About 200 m from the present shoreline, a 2–3 m-thick escarpment bank, abruptly interrupts the slight trending of the plain towards the lake. This morphological element, about 50 m from the archaeological site, is clearly delineated by the tree-line of eucalyptus, which were planted along the edge during the British Mandat (1920–1948 AD) in order to reclaim the areas facing the lake (Fig. 2A). Therefore, it is well established that the inner edge of the escarpment coincided with the lake level at the end of the 19th century.

## 3. Methods

The study was based on an integrated approach, involving (i) sedimentological and micropalaeontological (ostracods) analyses,

to obtain accurate depositional and palaeoenvironmental reconstructions, and (ii) geochemical analyses, to highlight potential pollution levels during the history of the harbour by means of anomalies in the trace metal contents. Three field campaigns were undertaken at Magdala and surrounding areas during the last two years. Detailed sedimentological and stratigraphic analyses were undertaken on three archaeological trenches (F18, F25 and F27 in Fig. 2) and a total of 25 samples were collected for laboratory analyses from the most representative sections (F18 and F25). These trenches, the location of which was based on georadar technology (Neal, 2004; Bini et al., 2010), are considered to be reference points because of their position close to the harbour structures (Fig. 2B). The sedimentary facies were described in terms of mean grain-size, color, sedimentary structures and other materials, including roots, wood fragments, vegetal debris, mollusk shells, osteological remains and anthropogenic artifacts (for the latter, the reader is referred to De Luca, 2010; Lena, 2012). The thickness of the individual sedimentary units was measured using a total station Leica TCR 305 via the Infrared EDM system with a standard prism GPH1-GPR1 and linked to an absolute altitude with accuracy of 10 mm + 2 ppm.

In order to define the sediment texture (Folk and Ward, 1957), grain size analyses were performed on samples of about 100 gg collected from F18 and F25. Each sample was dried to remove the moisture and then mechanically sieved. Samples from F18 and F25 were also analyzed for the ostracod fauna content, in order to improve facies characterization. About 100 g of dry sediments from each sample were soaked in water or, in case of cohesive sediments, water plus hydrogen peroxide (35% vol.), wet sieved through a 63 µm sieve (240 mesh) and then dried again in an oven for 24 h at 60 °C. Ostracods were observed under a binocular microscope and samples containing abundant and well-preserved valves were dry sieved through a 125 µm sieve to concentrate adult valves and to avoid problems about specific attribution of juvenile valves. In the >125 µm size fraction a semi-quantitative analysis of the ostracod fauna was performed, leading to the distinction of dominant and secondary species. The identification of species, their ecological significance and palaeoenvironmental interpretations of ostracod assemblages relied upon several reference works (Athersuch et al., 1989; Henderson, 1990; Meisch, 2000; Martens et al., 2002; Rosenfeld et al., 2004). Further information was also provided by comparison with the spatial distribution patterns of ostracods from the present-day Sea of Galilee and other Israel freshwater bodies (Mischke et al., 2010, 2012).

Geochemical analyses were performed with the aim to characterize the depositional facies in terms of metal contents, and thus to identify a possible anthropogenic contribution. The samples were analyzed using X-Ray Fluorescence (XRF) Spectrometry at Bologna University laboratories. The concentration of major elements was calculated using the method of Franzini et al. (1975), whilst the coefficients of Franzini et al. (1972), Leoni and Saitta (1976) and Leoni et al. (1982) were used for trace elements.

A reliable chronological framework for the studied sections was established integrating the archaeological findings with seven AMS <sup>14</sup>C dates performed at Poznan Radiocarbon Laboratory (Poland) on carbon-rich samples (mainly seeds, charcoal and gastropod shells belonging to the *Melanopsis* genus). Where possible, organic debris were preferred to gastropods, in order to avoid the reservoir effect, as stated by Lev et al. (2004, 2007) for *Melanopsis* shells from the Sea of Galilee. In the case of gastropod samples, the <sup>14</sup>C ages obtained from *Melanopsis* shells (<sup>14</sup>C age of coeval water) were matched with those from organic debris collected from the same stratigraphic horizon (samples F18-GS23\_w and F18-GS23\_m in Table 1). This led to an approximate reservoir age correction of 1375 years.

**Table 1**

Radiocarbon dates of the samples collected from the study sections F18, F25 and F27. Before calibration, conventional ages from *Melanopsis* shells were corrected for a reservoir age of ca. 1375 years, evaluated by comparison samples from the same horizon (F18-GS23\_w and F18-GS23\_m).

Section- sample code	Sampling depth (m bsl)	Lithofacies	Dated material	Conventional radiocarbon age (yr BP)	Calibrated age (2-sigma cal yr BP)	$\delta^{13}\text{C}$	Err.
F18-GS23_w	210.4	Backshore to upper shoreface sands	Wood fragments	2120 ± 29	2075 ± 76	-25.5	0.7
F18-GS23_m	210.4	Backshore to upper shoreface sands	<i>Melanopsis costata</i> shells	3496 ± 29	–	-0.2	0.4
F18-GS27	210.2	Lacustrine bay silty sands	Seeds	2059 ± 29	2033 ± 85	-20.5	0.5
F25-GS12	210.3	Lacustrine bay silty sands	Charcoal	2048 ± 29	2001 ± 70	-24.8	0.6
F27-GS6	210.3	Lacustrine bay silty sands	<i>Melanopsis costata</i> shells	3307 ± 31	1883 ± 64	-8.6	1.3
F27-2	210.1	Backshore to upper shoreface sands	<i>Melanopsis costata</i> shells	3483 ± 30	2073 ± 78	-0.1	0.3
F27-4	209.7	Backshore to upper shoreface sands	<i>Melanopsis costata</i> shells	3242 ± 30	1800 ± 77	3.5	0.2

Following correction of *Melanopsis* samples for the reservoir age, all radiocarbon data were calibrated using the calibration program CALIB 6.0 (referenced as Stuiver and Reimer, 1993) available at the website <http://calib.qub.ac.uk/calib/> and an adequate terrestrial dataset (IntCal09, Reimer et al., 2009). Calibrated ages (Table 1) were reported in this paper as the highest probability range (cal BP) obtained using two standard deviations (2-sigma).

## 4. Results

### 4.1. Sedimentology of the Magdala harbour archaeological site

Three main lithofacies associations (Figs. 4 and 5) were recognized in the study sections. These are described below in terms of sedimentary and geochemical features, ostracod contents and archaeological findings. Each lithofacies is related to a specific

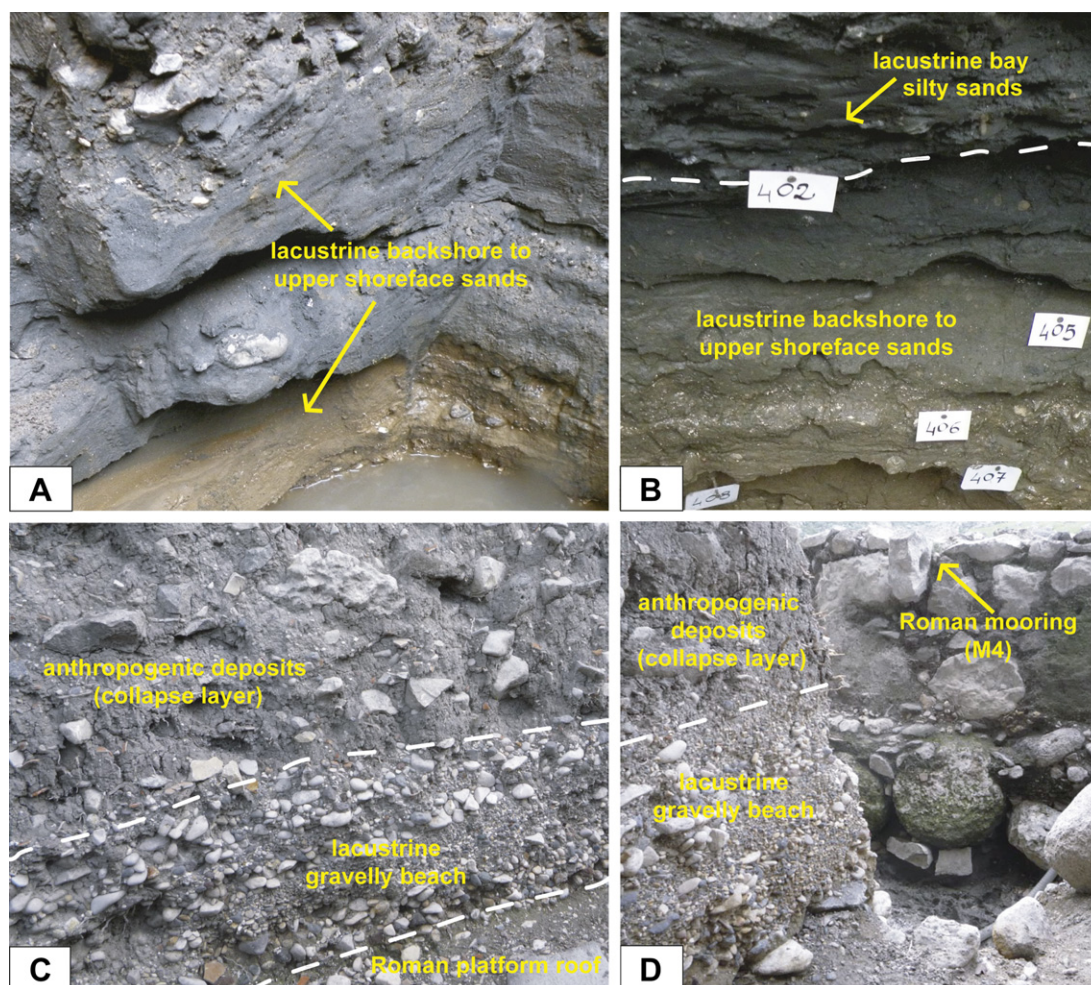


**Fig. 4.** Representative photographs depicting the three lithofacies associations identified in the Magdala harbour area and their relationships with the harbour structures and the anthropogenic deposits. (A) Lacustrine backshore to upper shoreface deposits showing an upward abrupt colour change from yellow to dark-grey (section F25). (B) Sharp boundary between foreshore/upper shoreface sands and lacustrine bay silty sands (section F18). The white dashed line marks the lithofacies transition. (C) Gravel beach deposits overlying the Roman platform roof. Note the evident clinostratification and clast imbrication dipping both towards the present shoreline (E–SE direction; left side of the figure). Anthropogenic deposits cap the succession (left side of trench F18). (D) Landward view of the Magdala harbour-abandonment succession (from the lakeshore towards inland), showing lateral relationships between the gravel layers and the Roman harbour structures. (For interpretation of the references to colour in this figure legend, the reader is referred to the web version of this article.)

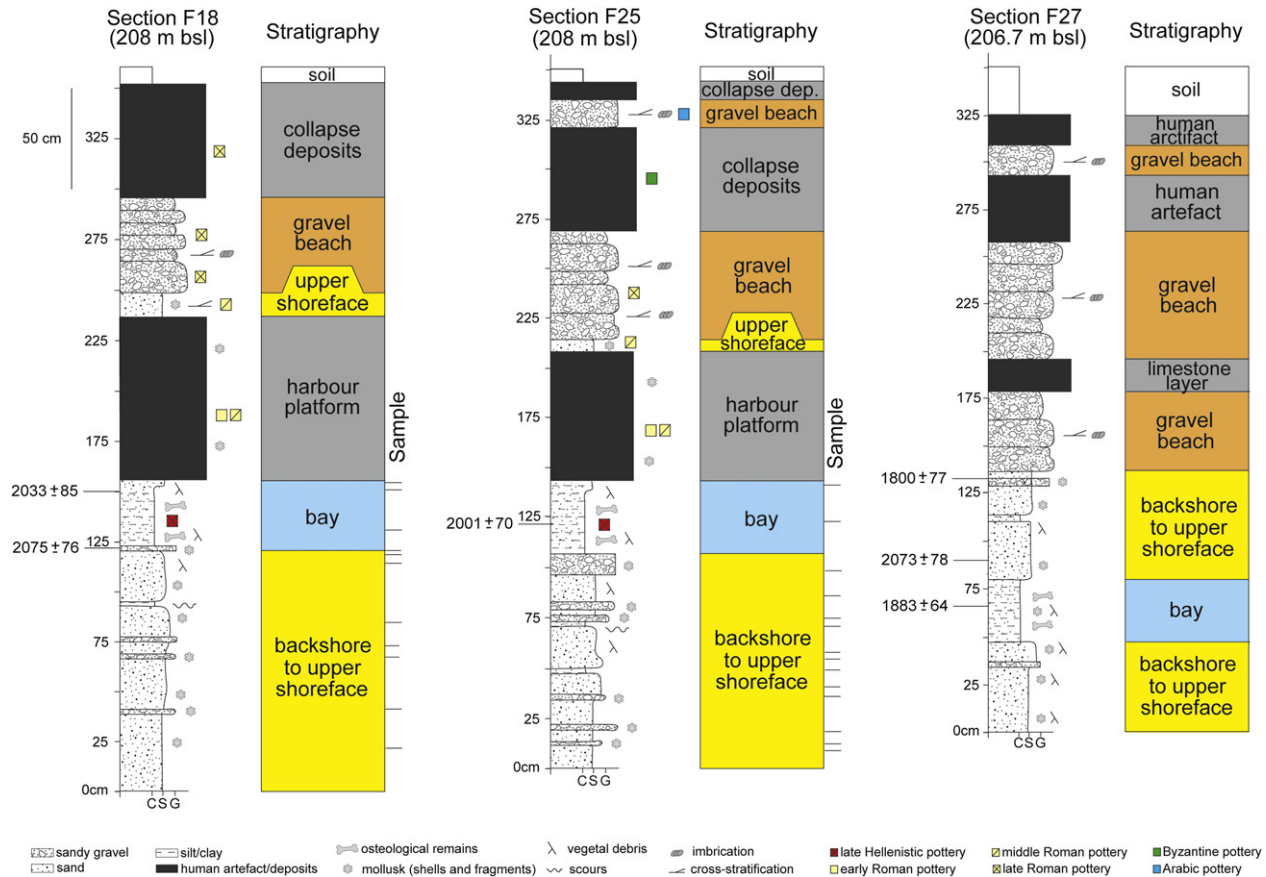


Fig. 5. Stratigraphy of F18, F25, and F27 sections (see Fig. 2 for location). Ages are reported as calibrated year BP.

depositional sub-environment of late Holocene age (Fig. 5). The lithofacies are locally interbedded with different types of artifacts and anthropogenic deposits, such as collapse debris, harbour structures, etc. To avoid repetitions in the description of the lithofacies, the data is presented from the base to the top, without describing each section individually. The diagnostic features of each lithofacies, including grain size, ostracods, and selected metal contents, are summarized in Table 2.

#### 4.1.1. Lacustrine backshore to upper shoreface sands

This lithofacies association, up to 1.25 m thick, consists of alternating yellow to dark-gray silty sands and moderately sorted sands (the sand fraction is commonly >80%), with lateral thickness variations and well preserved, abundant bivalve and gastropod shells, especially *Melanopsis* (Fig. 4A–B and 5). A well-developed, eastward dipping low-angle cross-lamination is locally observed and commonly associated to alignments of small (2–4 cm), well-

**Table 2**  
Diagnostic features of lithofacies as revealed by grain size, ostracods and selected metal determinations.

Lithofacies association	Grain size fraction (%)	Micropaleontological content	Metal concentration (mg/kg)
Lacustrine backshore to upper shoreface sands	Medium gravel: 0 ÷ 1.8 Fine gravel: 0 ÷ 5.9 Very fine gravel: 0 ÷ 4 Very coarse sand: 0 ÷ 4.4 Coarse sand: 0 ÷ 6.1 Medium sand: 2.5 ÷ 15.9 Fine sand: 36.9 ÷ 82.5 Very fine sand: 5 ÷ 39.7 Silt and clay: 0.6 ÷ 52.2	Abundant and oligotypic ostracod fauna. <i>Cyprideis torosa</i> (Jones, 1850) is the dominant species (87–100%) and is represented by both smooth and noded forms. As secondary species, rare valves of <i>Pseudocandona albicans</i> (Brady, 1868) (0.3–4.4%) and <i>Ilyocypris</i> spp. (0.3–1.8%) are encountered.	Copper: 15 ÷ 24 Lead: 0 ÷ 13 Zinc: 24 ÷ 44
Lacustrine bay silty sands	Medium gravel: 0 ÷ 0 Fine gravel: 0.2 ÷ 4.4 Very fine gravel: 0.2 ÷ 3.7 Very coarse sand: 0.3 ÷ 4.4 Coarse sand: 0.7 ÷ 5.8 Medium sand: 4.9 ÷ 22.1 Fine sand: 13.4 ÷ 36.3 Very fine sand: 20.5 ÷ 59.3 Silt and clay: 8 ÷ 29	Abundant and moderately diversified ostracod fauna. <i>Cyprideis torosa</i> is the dominant species (85–96%), mainly represented by noded forms. <i>Pseudocandona albicans</i> (2–7%) and <i>Ilyocypris</i> spp. (1.4–7.2%) occur as secondary species. Rare valves of <i>Eucypris virens</i> (Jurine, 1820), <i>Candonopsis parva</i> (Sywula, 1968) and <i>Heterocypris salina</i> (Brady, 1868) are also recorded (<1%).	Copper: 39 ÷ 58 Lead: 39 ÷ 85 Zinc: 59 ÷ 101

rounded discoidal pebbles made up of basalts, limestones and subordinate cherts. Discontinuous, 1–2 cm-thick dark-grey silty layers, showing minor load deformation structures, are occasionally observed. Vegetal debris and mollusk lags, a few centimeters thick and slightly dipping eastwards, are also recorded.

This lithofacies generally includes an abundant, well preserved oligotypic ostracod fauna predominantly represented by both smooth and noded forms of *Cyprideis torosa* (commonly more than 95%), which is a true euryhaline species able to tolerate very low salinity conditions down to 0.2‰ (Rosenfeld and Vesper, 1977). A few scattered valves of hypohaline ostracods (mainly *Pseudocandona albicans* and *Ilyocypris* species) are also encountered.

Concentrations of metals of potential anthropogenic origin from 16 sand samples display low values, narrowly constrained between 15 and 20 mg/kg for Cu, 24–33 mg/kg for Zn, and invariably <8 mg/kg (generally around 2 mg/kg) for Pb. Slightly higher values were observed within two silt intercalations (21–24 mg/kg for Cu, 44 mg/kg for Zn, and 8–13 mg/kg for Pb).

Scattered and not diagnostic pottery fragments are recorded within the uppermost part of this lithofacies association (sections F18 and F25). The archaeological findings testify to an occupation of the site apparently before the foundation of this portion of the city during the 3rd–2nd centuries BC (see also the radiocarbon age of ca. 2075 cal BP in F18; Fig. 5). This is also suggested from several assemblages found in other areas of the archaeological site (De Luca, 2010).

All these data suggest a relatively high-energy depositional environment, characterized by wave reworking and consistent with a lacustrine upper shoreface-foreshore/backshore setting developed in the Magdala area before ca. 2075 cal BP. The mollusk lags testify to storm events forming berms in the upper part of the foreshore. The thin and discontinuous, dark silty layers indicate abrupt and short-lived events of decreasing energy that affected backshore sub-environments, leading to deposition of fine-grained sediment through fall-out processes. The presence of small load structures could be related to rapid sedimentation of coarse-grained units, although seismically-induced deposition cannot be *a priori* ruled out. The homogeneously low metal values recorded within this lithofacies association are consistent with normal background concentrations for sandy deposits. The slightly higher metal contents observed within the silt intercalations reflect the characteristic positive correlation between trace metal concentration and the proportion of fine-grained material in sediments (Singh and Rajamani, 2001; Whitemore et al., 2004; Amorosi and Sammartino, 2007; Amorosi et al., in press).

#### 4.1.2. Lacustrine bay silty sands

This lithofacies association, 30–40 cm thick, is mainly composed of dark, poorly sorted fine to very fine sands with a high clay–silt fraction (up to 25%) and no evidence of sedimentary structures (Figs. 4B and 5). As a unique exception, rare lenticular, cm- to mm-thick silty sand layers with evidence of cross-lamination are recorded in the uppermost portion of this lithofacies association. Lamination is emphasized by foreset *laminae* made up of alternating dark-grey silty sand and organic vegetal debris. The abrupt boundary with the underlying lacustrine beach sands is commonly marked by an eastward-dipping, few cm-thick lag composed of mollusks and small pebbles (Fig. 5), showing a slight southward increase in thickness. Throughout the lithofacies association numerous vegetal debris, well preserved osteological remains (sheep, cattles) and mollusks are present. The abundant ostracod fauna, which is dominated by *Cyprideis torosa* (ranging between 85% and 95%), shows the highest species diversity of the entire sediment succession. The increase in species diversity is paralleled by a slight increase in the relative abundance of secondary species,

especially *Pseudocandona albicans* (2–7%) and *Ilyocypris* species (1.5–7%). The proportion of noded forms is extremely high relative to the smooth ones.

Concentrations of metals of potential anthropogenic origin from four clay samples yielded very high values, in the range of 39–58 mg/kg for Cu, 59–101 mg/kg for Zn, and 39–85 mg/kg for Pb.

A rich assemblage of archaeological artifacts including coins, glass and potsherds (De Luca, 2010; Lena, 2012) is also recorded. The findings include, amongst others, cooking ware of the type PENT 4, local amphorae of the types ANF 2, ANF 3, ANF 4 (according to the typology defined in Loffreda, 2008a, 2008b, 2008c), and imported pottery on the whole dating from the beginning of 2nd century BC up to the 1st century BC (Lena, 2012). In accordance with these data, the radiocarbon ages available from this lithofacies indicate an age of ca. 2030–2000 cal BP in F18 and F25, and 1880 cal BP in F27 (Fig. 5).

The sedimentological characteristics (dark colour, abundance of vegetal debris and lack of traction structures) and palaeontological features point to a semi-protected, low-energy depositional environment characterized by fall-out processes, high organic matter content and relatively low levels of oxygenation at the bottom. The exceptional abundance of osteological remains and archaeological artifacts, related to the Late Hellenistic period (Lena, 2012), suggests a depositional setting adjacent to an anthropized coastal area. This lithofacies association developed under strong anthropogenic forcing, as suggested by the anomalously high metal values, from two to six times higher than those from the underlying deposits (Table 2). Such high concentrations (especially Pb) cannot be thought as representing background values altered by simple grain size effects. On the basis of the archaeological findings, it is likely that these metal anomalies are related to concentration in sediment of nails (Cu), coins (Zn and Cu) and lead slag, such as net weights and oar handles.

#### 4.1.3. Lacustrine gravelly beach

This lithofacies association, up to 1.20 m thick, shows low-angle planar cross-bedding, wedge-shaped geometry and a slightly erosional lower boundary. It consists of vertically stacked, clast-supported clinostriated conglomerate layers dipping about 10° towards the E–SE (Fig. 4C–D and 5). These layers few decimeters thick, are well sorted (grain-size ranges from 1 to 4 cm) and show a marked eastward clast imbrication. Occasionally, thin fining-upward sequences are identified. Floated mollusk bioclasts and archaeological remains of Middle and Late Roman age (De Luca, 2010; Lena, 2012) have been observed, along with small vegetal debris. Clasts are mainly composed of limestones and subordinate basalts and cherts, reflecting composition of the surrounding wadi catchments. Clasts also display a high degree of roundness and are generally discoidal in shape. A sandy matrix, occasionally bearing bioclasts of *Melanopsis*, fills locally the intergranular pore space. No samples for micropalaeontological analysis were collected from these deposits, because of the very coarse grain-size, which precludes meiofauna preservation. Similarly, this unit was not sampled for geochemical analysis.

These features indicate proximity to the margin of an active fluvial mouth. Gravels were transported by the river to the lacustrine shore during high-energy flood events, being reworked by wave action to form a lacustrine gravel beach. This latter mainly records depositional environments ranging from the foreshore to the backshore.

#### 4.2. Stratigraphy of the harbour sections

Three of the ten trenches opened in front of the east side of the *quadriporticus* (Figs. 2 and 3) underwent an interdisciplinary



stratigraphic study. The harbour structure consists of two north-south juxtaposed docks, the older of which (Figs. 2 and 3) is late Hellenistic in age and displays two mooring stones *in situ*. The adjacent head-on dock is Roman in age; here, four mooring stones, a flight of steps, an east-west arm wharf and a platform slightly dipping towards the present-day shoreline, are preserved (Figs. 2B and 3). The stratigraphic description starts from section F18 (Fig. 5), since this trench provides a complete set of information. For details on the archaeological findings, the reader is referred to Lena (2012).

#### 4.2.1. Section F18

This section was opened against the east side of the Roman docks, in front of MS4 and MS5 and adjacent to the arm of the wharf (Figs. 2B and 3A, B). The lower part of the section exhibits a natural lacustrine shore succession, composed of yellow sands passing upwards to grayish sands (Figs. 4A and 5). One radiocarbon date from the top of these sands indicates an age of  $2075 \pm 76$  cal BP. Unfortunately, no diagnostic artifacts came from this unit. The sands are sharply overlain by a thin lenticular horizon made up of gravels and mollusks. Upwards, an abrupt transition to organic-rich, semi-protected lacustrine bay deposits is documented. This finer-grained stratigraphic unit is also characterized by many sheep and cattle bone splinters, as well as by the presence of many archaeological findings dated between the late 2nd century BC and the beginning of the 1st century BC. The pottery, along with the material collected inside the platform/slipway, dating back to the beginning of the 1st century AD (i.e., Late Hellenistic to Early Roman), provide a *terminus post quem* for the construction of the harbour structures. This is consistent with the radiocarbon age of  $2033 \pm 85$  cal BP obtained from the upper portion of the organic-rich unit (Fig. 5). The coins and few fragments of cast glass cups also point to the Late Hellenistic period (Lena, 2012).

As verified through some surveys (F8; F19; F31) against the inner side of the western wall of the *quadriporticus*, the foundation of the Hellenistic structures is partially placed on a basalt and limestone pebblework “buried” in this stratum.

The Roman piers, the slipway and the platform overlie the lacustrine bay succession. The platform, which slopes gently towards the lake, was erected using well-rounded pebble to heterometric rubble limestone and basalt clasts in addition to waste rocks. Sands containing mollusks have been observed between the clasts. The platform is overlapped by an eastward wedging thin layer of sandy foreshore to upper shoreface deposits bearing floated mollusks and potsherds and other findings, which date the phase of platform use to the Early-Middle Roman period (Lena, 2012). On the inner side of the platform, close to the dock, sands are replaced by an overlapping gravel beach shoreline succession containing scarce Late Roman pottery fragments. This sequence is interrupted by collapse layers of Late Roman age (Fig. 5).

#### 4.2.2. Section F25

This trench is located on the southern portion of the Roman quays, in front of the flight of stairs, about 15 m south of section F18 (Figs. 2B and 3B). The vertical stacking pattern of the depositional facies, as well as the archaeological content, are very similar to those described in section F18 (Fig. 5) and will not be reiterated here. The basal portion shows the sharp transition from lakeshore sandy deposits to low-energy, semi-protected bay sediments dated to  $2001 \pm 70$  cal BP (Fig. 5), on which the platform lays buried by sandy and gravel lacustrine shore deposits. A collapse layer, which can be physically correlated to the one identified at the top of section F18 (see Fig. 6), caps the sequence.

During the last archaeological campaign, in 2011, also the area between the two trenches was excavated. The resulting trench, 20 m-long and 3 m-wide, confirmed the overall stratigraphy, offering new insights into the post-Roman use of the area during the Late Byzantine (550–650 AD) and mid Islamic (650–1200 AD) ages.

#### 4.2.3. Section F27

This trench, which is located about 10 m east of section F25, is not physically connected to the harbour structures (Fig. 2B). The lower part of the section displays strong similarities with both sections F18 and F25, with sandy beach deposits overlain by lacustrine, semi-protected bay sediments. Upwards, a 50 cm-thick, upper shoreface sandy succession is overlain by three gravel beach layers, separated by anthropogenic deposits whose chronology is unclear at present. The lower layer is artificially cut and flattened by a pressed limestone layer, on which a floor, apparently Roman in age, was built (Fig. 5). Given a lake level between 209 and 210 m bsl during the Late Roman/Early Byzantine time (Hazan et al., 2005), the possible function of this pavement can be understood as a way to comply with the progradation of the coastline.

Above this floor a second gravel beach layer is observed, overlain in turn by a 30 cm-thick anthropogenic unit. Another thin gravel beach layer, overlain by an anthropogenic unit and a soil horizon, constitutes the top of the section. Three radiocarbon ages were performed on this section (Fig. 5): one within the lacustrine bay deposits ( $1883 \pm 64$  cal BP) and two in the overlying sandy deposits, approximately dating its base and top ( $2073 \pm 78$  cal BP;  $1800 \pm 77$  cal BP, respectively).

### 4.3. Stratigraphic correlations

In all the sections, the lacustrine backshore to upper shoreface sands constitute the lower part of the study succession, which is overlain by lacustrine, semi-protected bay silty sands. For F18 and F25 sections, this sequence is in turn overlain and slightly truncated by harbour structures (the arm of the platform's base and the quay foundation). By contrast, no correlative structures are present in F27, where natural lacustrine shoreface sands are recorded at the same elevation, overlapping the platform and the dock recorded in F18 and F25 (Fig. 6).

Although bay deposits represent an almost perfectly horizontal stratigraphic marker, with a lower boundary at an altitude of about 210.4 m bsl (Fig. 6), radiocarbon data suggest facies diachroneity between sections F18/F25 and F27. Specifically, in F27 the age of bay sediments is younger ( $1883 \pm 64$  cal BP) than the ages obtained from F18 and F25 ( $2033 \pm 85$  and  $2001 \pm 70$  cal BP, respectively). The date from the base of the overlying yellow sands in F27 ( $2073 \pm 78$  cal BP) is probably not reliable, being older than the age obtained from samples belonging to the lower bay stratigraphic level (Figs. 5 and 6). Moreover, the age of the bay stratigraphic level is consistent with the archaeological findings.

Upwards, the Roman slipway platform is buried, in both sections F18 and F25, by a thin lacustrine shore sandy deposit overlain by a conglomerate body at an altitude of between 209.32 and 209.42 m bsl. These deposits are also recorded above the quays.

Stratigraphic correlation between sections F18/F25 and section F27 is not readily apparent. It is likely that the upper sandy succession in F27, dated around  $1800 \pm 77$  cal BP, can be correlative with the thin sands of F18 and F25. Archaeological findings of Middle Roman age confirm this interpretation (Lena, 2012). It is reasonable to assume that the conglomerate body that overlies the uppermost sandy beach deposits identified in section F27 can be correlated, at least in part, with the conglomerate above the wharf arm in F18 and F25. In all sections, conglomerate layers alternating

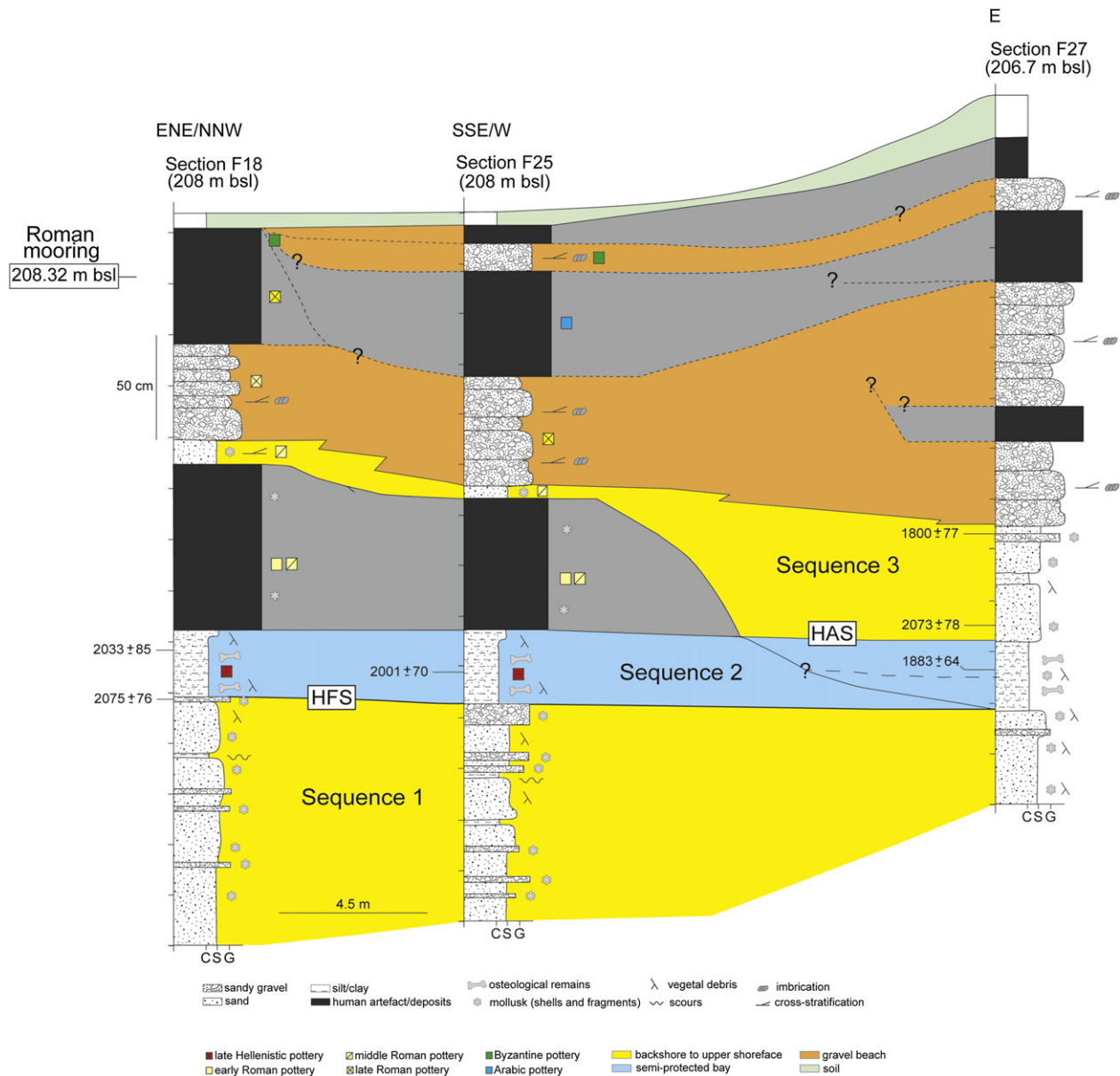


**Fig. 6.** Stratigraphic correlations between the study sections (F18, F25 and F27). Three thin sequences (pre-harbour, harbour and post-harbour sequences), corresponding to the three main evolutionary phases of the harbour area are shown (sequence 1–3). HFS: harbour foundation surface; HAS: harbour abandonment surface. Ages are reported as calibrated year BP.

with anthropogenic units form the uppermost portion of the succession (Fig. 6).

## 5. Magdala harbour history: natural and anthropogenic forcing factors

The stratigraphic relationships between lithofacies associations and the harbour structures identified at Magdala site, allow the distinction of three thin sedimentary sequences, reflecting different phases in the evolution of the harbour: 1) a pre-harbour foundation sequence, 2) a harbour sequence, and 3) a harbour-abandonment sequence (Fig. 6). Although further investigations are needed to get more robust conclusions, the abrupt boundary between sequences 1 and 2 is interpreted as the harbour foundation surface (HFS, *sensu* Marriner and Morhange, 2006, 2007), while the boundary between sequences 2 and 3 corresponds to the harbour abandonment surface (HAS *sensu* Marriner and Morhange, 2006, 2007).

### 5.1. Pre-harbour foundation sequence

This sequence (sequence 1 in Fig. 6), made up almost entirely of sands, underlies the harbour structures and records a relatively high-energy lacustrine backshore to upper shoreface setting characterized by almost continuous wave reworking. The transition from yellow to dark-grey sand (Fig. 4A) is tentatively related to a proto-harbour phase, although neither archaeological nor geochemical proxies, corroborating this hypothesis, were found. On the contrary, a subtle change in the ostracod content, corresponding to an increase in abundance of noded *Cyprideis torosa* with respect to the smooth type, was recognized at the transition from yellow to dark-grey colours. The pre-harbour sequence is abruptly cut at its top by the HFS. From an archaeological point of view, the first harbour facility was built in an area already characterized by the presence of human activity, most probably installed toward the slopes of Mt Arbel (Fig. 1).

## 5.2. HFS and harbour sequence

This sequence (sequence 2 in Fig. 6) is characterized by i) an abrupt change in grain size, from medium-coarse sand to silty sand; ii) a marked transition to dark-grey sediment colours, due to the high organic content and, likely, to a significant reduction of oxygenation at the basin bottom; iii) a change in the ostracod fauna, with an increase in species diversity and in the relative abundance of secondary taxa preferring stagnant waters; iv) a sudden and widespread appearance of potsherds, coins, bones and pieces of wood; and v) an abrupt increase in selected trace metals (Cu, Zn and Pb), which is consistent with anthropogenic pollution of the environment, probably linked to shipbuilding and boat insulation (see Sub-section 4.1.2). Samples collected from the overlying harbour platform provide consistent high metal concentrations, similar to (or slightly higher than) those recorded from the underlying bay sediments. Specifically, these values are in the range of 39–75 mg/kg for Cu, 70–114 mg/kg for Zn, and 55–117 for Pb (compare with Table 2).

The abrupt establishment of a low-energy depositional environment, no more strongly influenced by waves and characterized by settling processes, marks the replacement of a natural shore-lake environment by a populated semi-protected artificial lacustrine basin during the Late Hellenistic–Early Roman period. This implies an anthropogenic control on coastal sedimentation (anthropogenically forced sheltered basin; see Marriner and Morhange, 2007), related to human activities in the harbour area, testified by the discovery of the docks, mooring stones and arm of the wharf (Figs. 2 and 3). According to this interpretation, high pollution levels at the base of the HFS were induced by harbour activities and a dense human frequentation.

The harbour engineering techniques during the Late Hellenistic–Early Roman period were already advanced, as testified by the harbour structures including breakwaters built during the same period at Caesarea Maritima (west Israel) in an offshore area (e.g. Reinhardt and Raban, 1999). In this regard, it is plausible that the harbour was partially protected by a breakwater system, although a low-energy sedimentary environment could also be linked to jetties and quays (Morhange et al., 2003).

With regards to the archaeological data, the first structures (the port/tower and the *quadriporticus*) were associated with an urban settlement, of which considerable traces of houses and several artifacts survive in the western part of the site. The development and expansion of the harbour with the creation of the slipway/platform, the pier with mooring stones etc., dating around the mid-1st century AD, also correspond to the construction of large public buildings, such as the adjacent thermal bath complex. Even the street layout seems to have been extended in relation to the harbour.

A more complicated picture is attested by the stratigraphy of section F27, where the harbour bay deposits are younger and the overlying natural upper shoreface sands are in onlap onto the harbour structures. In accordance with recent archaeological excavations, which show two north-south juxtaposed moles (Figs. 2 and 3), these bay deposits may represent the waterfront lithofacies of the Roman docks. The younger quay, of Roman age, testifies to a reorganization of the harbour structures with a slight shift towards the lake (eastwards), in order to accommodate coastal progradation (Lena, 2012). This hypothesis is supported by the consistent age between the Roman quays and the harbour bay deposits (Fig. 6).

## 5.3. HAS and harbour-abandonment sequence

From the Middle Roman period onwards, the siltation and abandonment of the harbour are recorded (sequence 3 in Fig. 6).

The progressive burial of the platform occurred through deposition of upper shoreface-foreshore sands, followed by lake-beach conglomerates onto the Roman quay to about 30 cm away from the moorings (see Fig. 4D). The onlapping geometry between the conglomerate layers and the platform (Fig. 6) is in accordance with this interpretation, also in the relatively more distal section (see section F27 in Fig. 6).

The recurrent intercalation of natural lake-beach deposits with anthropogenic units suggests that after the final abandonment of the harbour a discontinuous human frequentation occurred, possibly related to small-scale lake-level fluctuations, occurred in the study area. This is apparent, for instance, from the two superimposed pavements, dated from the mid-Byzantine period (450–550 AD) to the Early Islamic I period (650–800 AD), and related to two distinct phases of occupation. These levels of use predate the level of natural lacustrine deposits above which, from the Early Islamic II, new structures were built, as revealed by the last excavation campaign. The sudden transition from sands to conglomerate layers may document important changes in sediment supply. These occurred after the Late Roman period and are possibly correlated to climatic changes from humid to arid phases and/or to tectonic events, such as the destructive earthquakes occurred in the of 363 AD and 749 AD (Marco et al., 2003).

From a socio-historical point of view, the siltation of the harbour coincided with a loss of interest in the maintenance of the harbour structure since the middle of the 3rd century AD. Simple facilities (see the platform in trench F27), were probably moved toward the new shoreline position, following coastal progradation. During Late Byzantine/Early Islamic times, a new, more rudimentary structure, 3 m lower than the Roman landing place, was probably built to serve the monastic settlement devoted to Mary Magdalene, as inferred by the ancient pilgrims' accounts (De Luca, 2010).

## 6. Conclusions

On the basis of an integrated geoarchaeological approach a new discovery at the Magdala harbour archaeological site has been outlined. The spatial variability of the depositional facies across the archaeological site has allowed us to reconstruct the sedimentary history of the Magdala harbour and to discern the natural to anthropogenic control on sedimentation. The Magdala site also represents a paradigm to define a template methodology for the future study of the coastal settlements along the Sea of Galilee.

Three thin sequences, corresponding to distinct evolutionary phases of the harbour, similar to those reported from other Mediterranean sites, have been reconstructed:

- 1) a *pre-harbour foundation phase*, characterized by the deposition of sands in a natural, lacustrine beach setting;
- 2) an *active harbour phase*, with the development of a semi-protected bay rich in osteological remains and archaeological artifacts. This phase reflects a strong anthropogenic control on coastal sedimentation during the harbour activity, also confirmed by the high levels of anthropogenic metal pollution. The harbour activity runs from the late Hellenistic to Middle Roman period;
- 3) a *harbour-abandonment phase*, which corresponds to the siltation and abandonment of the harbour and marks the end of the anthropogenic control on sedimentation, with return to natural sandy to conglomerate beach deposits.

## Acknowledgements

Our sincere thanks go to two anonymous reviews that strongly improved the manuscript. Thanks are also due to Prof. Goslar for

the useful discussions about radiocarbon data, and to the Magdala Project team for its support during the fieldwork. We are moreover indebted with Nick Marriner for his accurate English language revision.

## References

- Amiran, D.H.K., Arieh, E., Turcotte, T., 1994. Earthquakes in Israel and adjacent areas: macroseismic observations since 100 B.C.E. *Israel Exploration Journal* 44, 260–305.
- Amorosi, A., Sammartino, I., 2007. Influence of sediment provenance on background values of potentially toxic metals from near-surface sediments of Po coastal plain (Italy). *International Journal of Earth Sciences* 96, 389–396.
- Amorosi, A., Sammartino, I., Sarti, G. Background levels of potentially toxic metals from soils of the Pisa coastal plain (Tuscany, Italy) as identified from sedimentological criteria. *Environmental Earth Sciences*, in press, 12 pp.
- Athersuch, J., Horne, D.J., Whittaker, J.E., 1989. Marine and brackish water ostracods. In: Kermack, D.M., Barnes, R.S.K. (Eds.), *Synopses of the British Fauna (New Series)*, vol. 43. Brill E.J. Leiden, pp. 1–343.
- Bellotti, P., Calderoni, G., Di Rita, F., D'Orefice, M., D'Amico, C., Esu, D., Magri, D., Preite Martinez, M., Tortore, P., Valeri, P., 2011. The Tiber river delta plain (central Italy): coastal evolution and implications for the ancient Ostia Roman settlement. *The Holocene* 21, 1105–1116.
- Bini, M., Chelli, A., Durante, A., Gervasini, L., Pappalardo, M., 2009. Geoarchaeological sea-level proxies from a silted up harbour: a case study of the Roman colony of Luni (Northern Tyrrhenian Sea, Italy). *Quaternary International* 206 (1–2), 70–78.
- Bini, M., Fornaciari, A., Ribolini, A., Bianchi, A., Sartini, S., Coschino, F., 2010. Medieval phases of settlement at Benabbi castle, Apennine mountains, Italy: evidence from ground penetrating radar survey. *Journal of Archaeological Sciences* 37, 3059–3067.
- Bini, M., Bruckner, H., Chelli, A., Da Prato, S., Gervasini, L., 2012. Palaeogeographies of the Magra Valley coastal plain to constrain the location of the Roman harbour of Luna (NW Italy). *Palaeogeography, Palaeoclimatology, Palaeoecology* 337–338, 37–51.
- Bisson, M., Bini, M., 2012. A multidisciplinary approach to reveal palaeo-hydrographic features: the case study of Luna archaeological site surroundings. *International Journal of Geographical Information Science* 26, 327–343.
- Blue, L., Khalil, E. (Eds.), 2010. *Lake Mareotis: Reconstructing the Past*. Proceedings of the International Conference on the Archaeology of the Mareotic Region Held at Alexandria University, Egypt, 5th–6th April 2008. *Bar International Series* 2113, vol. 2. University of Southampton Series in Archaeology, Oxford, 156 pp.
- Bony, G., Marriner, N., Morhange, C., Kaniewski, D., Perinçek, D., 2012. A high-energy deposit in the Byzantine harbour of Yenikapi, Istanbul (Turkey). *Quaternary International* 266, 117–130.
- Bruckner, H., Müllenhoff, M., Handl, M., van der Borg, K., 2002. Holocene landscape evolution of the Büyük Menderes alluvial plain in the environs of Myous and Priene (western Anatolia, Turkey). *Zeitschrift für Geomorphologie N.F.* 127, 47–65.
- De Luca, S., 2010. La città ellenistica-romana di Magdala/Taricheae. Gli scavi del Magdala Project 2007 e 2008: relazione preliminare e prospettive di indagine. *Liber Annus* 49, 343–562.
- De Luca, S., 2012. Scoperte archeologiche recenti attorno al Lago di Galilea: contributo alla studio dell'ambiente del Nuovo Testamento e del Gesù storico. In: Paximadi, G., Fidanio, M. (Eds.), *Terra Sancta: archeologia ed esegesi. Atti dei convegni 2008–2010*, ISCA Serie Archeologica 1 (Lugano 2012), pp. 1–58.
- De Luca, S., "Urban development of the city of Magdala/Taricheae in the light of the New Excavations: remains, problems and perspectives", Symposium Greco-Roman Galilee (21st–23rd June 2009, Tel Hai Academic College – Kinneret College – Macalester College – Carthage College), in press.
- De Luca, S., Lena, A. The Harbor of the City of Magdala/Taricheae on the shores of the Sea of Galilee, from the Hellenistic to the Byzantine times. New discoveries and preliminary results. In: *Harbors and Harbor Cities in the Eastern Mediterranean from Antiquity to Byzantium. Recent Discoveries & New Approaches*. Istanbul 30/5, 1/6 2011, in press.
- Devillers, B., 2008. Holocene Morphogenesis and Land Use in a Semi-arid Watershed, The Gialias River, Cyprus. *British Archaeological Report – Archaeopress*, Oxford, p. 199.
- Feuser, S., 2011. The roman harbour of Alexandria Troas, Turkey. *The International Journal of Nautical Archaeology* 40 (2), 256–273.
- Flaux, C., Morhange, C., Marriner, N., Rouchy, J.M., 2011. Bilan hydrologique et bio-sédimentaire de la lagune du Maryût (delta du Nil, Egypte) entre 8000 et 3200 ans cal. B.P. *Geomorphologie: relief, processus, environnement* 3, 261–278.
- Flaux, C., Marriner, N., el-Assal, M., Morhange, C., Rouchy, J.M., Soulié-Marsche, I., Torab, T., 2012. Environmental changes in the Maryut lagoon (western Nile delta) during the last ~2000 years. *Journal of Archaeological Science* 39 (12), 3493–3504.
- Folk, R.L., Ward, W., 1957. Brazos River bar: a study in the significance of grain size parameters. *Journal of Sedimentary Petrology* 27, 3–26.
- Franzini, M., Leoni, L., Saitta, M., 1972. A simple method to evaluate the matrix effects in X-ray fluorescence analysis. *X-Ray Spectrometry* 1, 151–154.
- Franzini, M., Leoni, L., Saitta, M., 1975. Revisione di una metodologia analitica per fluorescenza-X basata sulla correzione completa degli effetti di matrice. *Rendiconti della Società italiana di mineralogia e petrologia* 31, 365–378.
- Galili, E., Rosen, B., Boaretto, E., Tzatzkin, S., 2007. Kursi Beach Final Report, HA-ES, 119, 2007. <[http://www.hadashot-esi.org.il/report\\_detail\\_eng.asp?id=508&mag\\_id=112](http://www.hadashot-esi.org.il/report_detail_eng.asp?id=508&mag_id=112)> (31.12.11).
- Giraudi, C., Tata, C., Paroli, L., 2009. Late Holocene evolution of Tiber River Delta and Geoarchaeology of Claudius and Trajan Harbour, Rome. *Geoarchaeology an International Journal* 24 (3), 371–382.
- Goiran, J.P., Tronchere, H., Salomon, F., Carbonel, P., Djerbi, H., Ognard, C., 2010. Palaeoenvironmental reconstruction of the ancient harbours of Rome: Claudius and Trajan's marine harbours on the Tiber delta. *Quaternary International* 216, 3–13.
- Goodman, B.V., Reinhardt, E.G., Dey, H.W., Boyce, J.I., Schwarcz, H.P., Sahouglu, V., Erkanal, H., Artzy, M., 2009. Multi-proxy geoarchaeological study redefines understanding of the palaeocoastlines and ancient harbours of Liman Tepe (Iskele, Turkey). *Terra Nova* 21 (2), 97–104.
- Guidoboni, E., 1994. *Catalogue of Ancient Earthquakes in the Mediterranean Area up to the 10th Century*. Istituto Nazionale di Geofisica, Rome, 504 pp.
- Hakanson, L., Parparov, A., Hambright, K.D., 2000. Modelling the impact of water level fluctuations on water quality (suspended particulate matter) in Lake Kinneret, Israel. *Ecological Modelling* 128, 101–125.
- Hazan, N., Steinb, M., Agnon, A., Marco, S., Nadel, D., Negendank, J.F.W., Schwab, M.J., Neev, D., 2005. The late Quaternary limnological history of Lake Kinneret (Sea of Galilee), Israel. *Quaternary Research* 63, 60–77.
- Hambright, K.D., Eckert, W., Leavitt, P.R., Schelske, C.L., 2004. Effects of historical lake level and land use on sediment and phosphorus accumulation rates in Lake Kinneret. *Environmental Science & Technology* 38, 6460–6467.
- Henderson, P.A., 1990. Freshwater ostracods. In: Kermack, D.M., Barnes, R.S.K. (Eds.), *Synopses of the British Fauna (New Series)*, vol. 42. Brill E.J. Leiden, p. 228.
- Kraft, J.C., Rapp, G.R., Kayan, I., Luce, J.V., 2003. Harbour areas at ancient Troy: sedimentology and geomorphology complement Homer's Iliad. *Geology* 31, 163–166.
- Lena A., 2012. Il porto di Magdala/Tarichea sul Lago di Galilea. PhD thesis in "Archaeology: East-West Relations", PhD Program in Intercultural Studies, Università di Napoli "L'Orientale", Napoli 2012, (unpublished) 247 pp.
- Leoni, L., Saitta, M., 1976. X-ray fluorescence analysis of 29 trace elements in rock and mineral standard. *Rendiconti della Società italiana di mineralogia e petrologia* 32, 497–510.
- Leoni, L., Menichini, M., Saitta, M., 1982. Determination of S, Cl and F in silicate rocks by X-ray fluorescence analysis. *X-Ray Spectrometry* 11, 156–158.
- Lev, L., Boerretto, E., Marco, S., Stein, M., 2004. Assessment of the Potential Use of Melanopsis Shells as Paleo-environmental Chronometer. Annual Meeting – Israel Geological Society.
- Lev, L., Boerretto, E., Heller, J., Marco, S., Stein, M., 2007. The feasibility of using *Melanopsis* shells as radiocarbon chronometers, Lake Kinneret, Israel. *Radiocarbon* 49, 1003–1115.
- Loffreda, S., 2008a. Cafarnao VI: Tipologie e contesti stratigrafici della ceramica (1968–2003), SBF Collectio Maior 48 (Jerusalem 2008), 396 pp.
- Loffreda, S., 2008b. Cafarnao VII: Documentazione grafica della ceramica (1968–2003), SBF Collectio Maior 49 (Jerusalem 2008), 346 pp.
- Loffreda, S., 2008c. Cafarnao VIII: Documentazione fotografica degli oggetti, SBF Collectio Maior 50 (Jerusalem 2008), 151 pp.
- Marco, S., Hartal, M., Hazan, N., Lev, L., Stein, M., 2003. Archaeology, history, and geology of the A.D. 749 earthquake, Dead Sea transform. *Geology* 31, 665–668.
- Marriner, N., Morhange, C., 2005. Under the city centre, the ancient harbour. Tyre and Sidon: heritages to preserve. *Journal of Cultural Heritage* 6, 183–189.
- Marriner, N., Morhange, C., 2006. The Ancient Harbour Parasequence: anthropogenic forcing of the stratigraphic highstand record. *Sedimentary Geology* 186, 13–17.
- Marriner, N., Morhange, C., 2007. Geoscience of ancient Mediterranean harbours. *Earth-Science Reviews* 80, 137–194.
- Marriner, N., Morhange, C., Boudagher-Fadel, M., Bourcier, M., Carbonel, P., 2005. Geoarchaeology of Tyre's ancient ern harbour, Phoenicia. *Journal of Archaeological Science* 32, 1302–1327.
- Marriner, N., Morhange, C., Doumet-Serhal, C., 2006. Geoarchaeology of Sidon's ancient harbours, Phoenicia. *Journal of Archaeological Science* 33, 1514–1535.
- Marriner, N., Morhange, C., Saghih-Beydoun, M., 2008. Geoarchaeology of Beirut's ancient harbour, Phoenicia. *Journal of Archaeological Science* 35, 2495–2516.
- Marriner, N., Morhange, C., Borschneck D., Flaux, C. Holocene sedimentary sources in southern Lebanon, Eastern Mediterranean. *Quaternary International*, in press.
- Martens, K., Schwartz, S.S., Meisch, C., Blaustein, L., 2002. Nonmarine Ostracoda (Crustacea) of Mount Carmel (Israel), with taxonomic notes on Eucypridinae and circum-mediterranean *Heterocypris*. *Israel Journal of Zoology* 48, 53–70.
- Meisch, C., 2000. *Freshwater Ostracoda of Western and Central Europe*. Spektrum, Heidelberg, 522 pp.
- Mischke, S., Almogi-Labin, A., Ortal, R., Rosenfeld, A., Schwab, M.J., Boomer, I., 2010. Quantitative reconstruction of lake conductivity in the Quaternary of the Near East (Israel) using ostracods. *Journal of Paleolimnology* 43, 667–688.
- Mischke, S., Ginat, H., Al-Saqarat, B., Almogi-Labin, A., 2012. Ostracods from water bodies in hyperarid Israel and Jordan as habitat and water chemistry indicators. *Ecological Indicators* 14, 87–99.
- Morhange, C., Goiran, J.P., Bourcier, M., Carbonel, P., Le Campion, J., Rouchy, J.M., Yon, M., 2000. Recent Holocene paleo-environmental evolution and coastline changes of Kition, Larnaca, Cyprus, Mediterranean Sea. *Marine Geology* 170, 205–230.

- Morhange, C., Laborel, J., Hesnard, A., 2001. Changes of relative sea level during the past 5000 years in the ancient harbour of Marseilles, Southern France. *Palaeogeography, Palaeoclimatology, Palaeoecology* 166, 319–329.
- Morhange, C., Blanc, F., Schmitt-Mercury, S., Bourcier, M., Carbonel, P., Oberlin, C., Prone, A., Vivent, D., Hesnard, A., 2003. Stratigraphy of late-Holocene deposits of the ancient harbour of Marseilles, southern France. *The Holocene* 13 (4), 593–604.
- Neal, A., 2004. Ground-penetrating radar and its use in sedimentology: principles, problems and progress. *Earth-Science Reviews* 66, 261–330.
- Neev, D., Emery, E.O., 1967. The Dead Sea. *Geological Survey of Israel Bulletin* 41, 1–147.
- Nishri, A., Stiller, M., Rimmer, A., Geifman, Y., Krom, M., 1999. Lake Kinneret (The Sea of Galilee): the effects of diversion of external salinity sources and the probable chemical composition of the internal salinity sources. *Chemical Geology* 158, 37–52.
- Nun, M., 1987. Ancient Ports and Harbours in the Kinneret. Ariel, Jerusalem, 32 pp.
- Nun, M., 1988. Ancient Anchorage and Harbours Around the Sea of Galilee. Kinneret Sailing Co., Ein. Gev., Israel, 31 pp.
- Pan, H., Avissar, R., Haidvogel, D.B., 2002. Summer circulation and temperature structure of Lake Kinneret. *Journal of Physical Oceanography* 32, 295–313.
- Raban, A., 1988. The boat of Migdal Nunia and the anchorages of the Sea of Galilee from the time of Jesus. *The International Journal of Nautical Archaeological and Underwater Exploration* 17 (4), 311–329.
- Reimer, P.J., Baillie, M.G.L., Bard, E., Bayliss, A., Beck, J.W., Blackwell, P.G., Bronk Ramsey, C., Buck, C.E., Burr, G.S., Edwards, R.L., Friedrich, M., Grootes, P.M., Guilderson, T.P., Hajdas, I., Heaton, T.J., Hogg, A.G., Hughen, K.A., Kaiser, K.F., Kromer, B., McCormac, F.G., Manning, S.W., Reimer, R.W., Richards, D.A., Southon, J.R., Talamo, S., Turney, C.S.M., van der Plicht, J., Weyhenmeyer, C.E., 2009. INTCAL 09 and MARINE09 radiocarbon age calibration curves, 0–50,000 years Cal BP. *Radiocarbon* 51, 1111–1150.
- Reinhardt, E.G., Patterson, R.T., Schröder-Adams, C.J., 1994. Geoarchaeology of the ancient harbour site of Caesarea Maritima, Israel: evidence from sedimentology and palaeoecology of benthic foraminifera. *Journal of Foraminiferal Research* 24, 37–48.
- Reinhardt, E.G., Patterson, R.T., Blenkinsop, J., Raban, A., 1998. Palaeoenvironmental evolution of the inner basin of the ancient harbour at Caesarea Maritima, Israel: foraminiferal and Sr isotopic evidence. *Revue de Palaeobiologie* 17, 1–21.
- Reinhardt, E.G., Raban, A., 1999. Destruction of Herod the Great's harbor at Caesarea Maritima, Israel – Geoarchaeological evidence. *Geology* 27, 811–814.
- Rosenfeld, A., Vesper, B., 1977. The variability of sieve-type pores in *Cyprideis torosa* (Jones 1850), recent and fossil, as an indicator for salinity and palaeosalinity. In: Loffler, H., Danielopol, D. (Eds.), *Aspects of Ecology and Zoogeography of Recent and Fossil Ostracoda: The Hague*, pp. 55–66.
- Rosenfeld, A., Nathan, Y., Feibel, C.S., Schildman, B., Halicz, L., Goren-Inbar, N., Siman-Tov, R., 2004. Palaeoenvironment of the Acheulian Gesher Benot Ya'aqov Pleistocene lacustrine strata, ern Israel—lithology, ostracod assemblages and ostracod shell geochemistry. *Journal of African Earth Sciences* 38, 169–181.
- Russell, K.E., 1985. The earthquake chronology of Palestine and west Arabia from the 2nd through the mid-8th century A.D. *American School of Oriental Research Bulletin* 260, 37–60.
- Singh, P., Rajamani, V., 2001. Geochemistry of the floodplain sediments of the Kaveri River, southern India. *Journal of Sedimentary Research* 71, 50–60.
- Sivan, D., Wdowinski, S., Lambeck, K., Galili, E., Raban, A., 2001. Holocene sea-level changes along the Mediterranean coast of Israel, based on archaeological observations and numerical model. *Palaeogeography, Palaeoclimatology, Palaeoecology* 167, 101–117.
- Stein, M., 2001. The sedimentary and geochemical record of Neogene–Quaternary water bodies in the Dead Sea Basin—inferences for the regional palaeoclimatic history. *Journal of Palaeolimnology* 26, 271–282.
- Stuiver, M., Reimer, P.J., 1993. Extended  $^{14}\text{C}$  data base and revised CALIB 3.0  $^{14}\text{C}$  age calibration program. *Radiocarbon* 35 (1), 215–230.
- Whitemore, G.P., Crook, K.A., Johnson, D.P., 2004. Grain size control of mineralogy and geochemistry in modern river sediment, New Guinea collision, Papua New Guinea. *Sedimentary Geology* 171 (1–4), 129–157.